Modeling Tight Junction Dynamics and Oscillations

Fuad Kassab, Jr.,[1] Ricardo Paulino Marques,[1] and Francisco Lacaz-Vieira[2]

[1]Escola Politécnica, Departamento de Engenharia de Telecomunicaçoes e Controle, and [2]Departmento de Fisiologia e Biofísica, Instituto de Ciencias Biomédicas, Universidade de São Paulo, 05508-900 São Paulo, Brazil

ABSTRACT Tight junction (TJ) permeability responds to changes of extracellular Ca^{2+} concentration. This can be gauged through changes of the transepithelial electrical conductance (G) determined in the absence of apical Na^{+}. The early events of TJ dynamics were evaluated by the fast Ca^{2+} switch assay (FCSA) (Lacaz-Vieira, 2000), which consists of opening the TJs by removing basal calcium (Ca^{2+}_{bl}) and closing by returning Ca^{2+}_{bl} to normal values. Oscillations of TJ permeability were observed when Ca^{2+}_{bl} is removed in the presence of apical calcium (Ca^{2+}_{ap}) and were interpreted as resulting from oscillations of a feedback control loop which involves: (a) a sensor (the Ca^{2+} binding sites of zonula adhaerens), (b) a control unit (the cell signaling machinery), and (c) an effector (the TJs). A mathematical model to explain the dynamical behavior of the TJs and oscillations was developed. The extracellular route (ER), which comprises the paracellular space in series with the submucosal interstitial fluid, was modeled as a continuous aqueous medium having the TJ as a controlled barrier located at its apical end. The ER was approximated as a linear array of cells. The most apical cell is separated from the apical solution by the TJ and this cell bears the Ca^{2+} binding sites of zonula adhaerens that control the TJs. According to the model, the control unit receives information from the Ca^{2+} binding sites and delivers a signal that regulates the TJ barrier. Ca^{2+} moves along the ER according to one-dimensional diffusion following Fick's second law. Across the TJ, Ca^{2+} diffusion follows Fick's first law. Our first approach was to simulate the experimental results in a semiquantitative way. The model tested against experiment results performed in the frog urinary bladder adequately predicts the responses obtained in different experimental conditions, such as: (a) TJ opening and closing in a FCSA, (b) opening by the presence of apical Ca^{2+} and attainment of a new steady-state, (c) the escape phase which follows the halt of TJ opening induced by apical Ca^{2+}, (d) the oscillations of TJ permeability, and (e) the effect of Ca^{2+}_{ap} concentration on the frequency of oscillations.

KEY WORDS: calcium • tight junctions • cell adhesion • models, theoretical • calcium-binding proteins

INTRODUCTION

The frog urinary bladder wall consists of epithelium, submucosa, and serosa. The mucosal (or apical or luminal) surface is outlined with epithelial cells disposed in a single layer showing a thickness of ~10 μM. The submucosa is made of a delicate stroma of fibroblasts and collagen fibers, blood and lymph vessels, nerves, and smooth muscle bundles. The serosa is a continuous layer of flat cells, the peritoneal or serosal membrane (mesothelial cells). For a review of amphibian urinary bladder ultrastructure see Choi (1963).

In a series of previous studies (Castro et al., 1993; Lacaz-Vieira and Kachar, 1996; Lacaz-Vieira, 1997, 2000; Lacaz-Vieira et al., 1999; Lacaz-Vieira and Jaeger, 2001) it was shown that in epithelial membranes the dynamics of tight junction (TJ)* opening and closing can be studied in short-term experiments (a condition in which many of the later regulatory phenomena can be prevented) by using the fast Ca^{2+} switch assay (FCSA). This assay consists in opening the TJs by removing Ca^{2+} from the basal solution (Ca^{2+}_{bl}) and subsequently closing the junctions by returning Ca^{2+} to the basal solution. The time courses of TJ opening and closing in an FCSA were shown to approximately follow single exponential time courses both in the natural epithelia of the frog urinary bladder (Lacaz-Vieira, 2000) as well as in A6 cell monolayers (Lacaz-Vieira and Jaeger, 2001). Manipulations of Ca^{2+}_{ap} during the FCSA, both in concentration and the moment Ca^{2+}_{ap} is changed, can markedly affect the dynamics of the TJs, blocking the opening process, slowing down its time course (Lacaz-Vieira, 1997), or inducing a periodic phenomena characterized by oscillations of tissue electrical conductance (G) (Lacaz-Vieira, 2000).

In the absence of apical Na^{+}, G is a reliable estimate of the paracellular permeability, which is mainly determined by the TJ (Castro et al., 1993; Lacaz-Vieira and Kachar, 1996). A large number of papers deals with the role of cell signaling systems on the control of TJ opening and closing (for reviews see Cereijido et al., 1988, 2000; Balda et al., 1992; Schneeberger and Lynch, 1992; Hopkins et al., 2000; Kniesel and Wolburg, 2000;

Address correspondence to Francisco Lacaz-Vieira, Departmento de Fisiologia e Biofísica, Instituto de Ciencias Biomédicas, Universidade de São Paulo, 05508-900 São Paulo, Brazil. Fax: (55) 11-3091.7285; E-mail: flacaz@usp.br

*Abbreviations used in this paper: ER, extracellular route; FCSA, fast Ca^{++} switch assay; L, length of ER; R, transepithelial electrical resistance, in Ω cm²; SSC, short-circuit current; TJ, tight junction.

J. Gen. Physiol. © The Rockefeller University Press • 0022-1295/2002/08/237/11 $5.00
Volume 120 August 2002 237–247
http://www.jgp.org/cgi/doi/10.1085/jgp.20028604

Turner, 2000; Walsh et al., 2000). In particular, the PKC plays a key role in TJ opening in response to extracellular Ca^{2+} withdrawal without major effects on the reverse process of TJ closing (Lacaz-Vieira, 2000). PKC inhibition by H7 not only prevents TJ opening in response to basal Ca^{2+} removal, but induces a prompt blockade of TJ oscillations induced by apical Ca^{2+}, oscillations that reappear when H7 is removed (Lacaz-Vieira, 2000).

Understanding the dynamic process of TJ opening and closing in response to the extracellular levels of Ca^{2+} concentration, as well as the role of signaling systems, can be greatly facilitated through mathematical modeling of the behavior of the TJs. In this paper we studied the properties of a mathematical model in which the TJ barrier is controlled by the Ca^{2+} levels at the Ca^{2+} binding sites of zonula adhaerens (Gumbiner et al., 1988). In particular, the conclusions reached from the analysis of this model support our previous hypothesis that oscillations of G which occur in response to a step rise of apical Ca^{2+} concentration in a FCSA result from oscillatory opening and closing of the TJ barrier (Lacaz-Vieira, 2000).

MATERIALS AND METHODS

Urinary bladders of the frog *Rana catesbeiana* were used. Animals were anesthetized by subcutaneous injection of a 2% solution of 3-aminobenzoic acid ethyl ester (methanesulfonate salt) (Sigma-Aldrich) at a dose of 1 ml/100 g of body weight. Experiments were conducted in accordance with the The Guide for the Care and Use of Laboratory Animals. The abdominal cavity was opened, a cannula was passed through the cloaca and the urinary bladder was inflated with 15–20 ml of air according to the animal size. Plastic rings of 20 mm diameter were glued to the serosal surface of the bladder with ethylcyanoacrylate adhesive (Pronto CA8, 3M, or Super Bonder; Loctite). The fragment of tissue framed by the plastic ring was excised and immersed in Ringer's solution. Subsequently, it was mounted in a modified Ussing's chamber (Castro et al., 1993), exposing an area of 0.5 cm^2. Hemichambers with recessed rims filled with high viscosity silicone grease (high vacuum grease; Dow Corning) prevented tissue edge damage (Lacaz-Vieira, 1986). Each chamber compartment was perfused with a continuous flow of solution (up to 25 ml/min) driven by gravity from reservoirs through plastic tubings. Unstirred layers on the surfaces of the tissue were minimized, but not eliminated, by directing the incoming fluid toward the tissue surfaces. Each compartment was drained through a spillway open to the atmosphere, so that the pressure inside each compartment was kept fairly constant at the atmospheric level. Rapid solution changes were obtained without interruption of voltage clamping by switching the inlet tubings at their connections with the chamber.

Solutions

Unless otherwise stated, the inner bathing solution was NaCl Ringer's solution with the following composition (in mM): NaCl-Ringer, NaCl 115, $KHCO_3$ 2.5, and $CaCl_2$ 1.0. The apical bathing fluids were simple salt solutions, nonbuffered, prepared with glass distilled water with pH around 6.0, and free-Ca^{2+} concentration in the range of 1.5×10^{-7} and 2.0×10^{-7} M (Castro et al., 1993). The apical solution was KCl 75 mM to eliminate Na^+, in order to rule out any contribution of a transcellular Na^+ conductance to the overall tissue electrical conductance. No EGTA was used in the bathing solutions since this chelating agent diffusing into the lateral spaces affects the time course of Ca^{2+} concentration increase or decrease in this region in response to changes of Ca^{2+} concentration in the bathing solutions.

Electrical Measurements

A conventional analogue voltage-clamp (WPI DVC 1000) was used. Saturated calomel half-cells with 3 M KCl-agar bridges were used to measure the electrical potential difference across the skin. Current was passed through Ag-AgCl 3 M KCl electrodes and 3 M KCl-agar bridges, adequately placed to deliver a uniform current density across the skin. The clamping current was continuously recorded by a strip-chart recorder. Clamping current and voltage were also digitized through an analogue-to-digital converter at a digitizing rate of 100 Hz (Digidata 1200 and Axotape 2.0; Axon Instruments, Inc.) and stored in a computer for further processing.

Chemicals

All chemicals were obtained from Sigma-Aldrich.

Statistics

The results are presented as mean ± SEM. Comparisons were performed using Student's paired *t* test. (Neter and Wasserman, 1974).

FCSA

Tissues were bathed in nominally Ca^{2+}-free apical solution. The TJs were opened by removal of Ca^{2+} from the basal solution, inducing an increase of the overall tissue electrical conductance (G). Subsequent resealing of the TJs was induced by reintroducing Ca^{2+} into the basal fluid, causing a decrease of G toward initial control levels.

Simulation

Simulation of TJ dynamics was performed in a PC computer using MATLAB® technical computing environment and Simulink® a MATLAB tool for modeling, simulating, and analyzing physical and mathematical systems.

RESULTS

The Model

The mathematical model we are about to build aims to interpret the dynamics of TJ opening and closing in response to changes of the Ca^{2+} concentration in the bathing solutions, a procedure known as FCSA (Lacaz-Vieira, 1997, 2000; Lacaz-Vieira et al., 1999; Lacaz-Vieira and Jaeger, 2001). Our initial goal in modeling was not only to interpret the dynamics of TJ opening and closing in an FCSA but to understand the origin of oscillations of TJ permeability that are observed in some conditions during a FCSA experiments (Lacaz-Vieira, 2000). The basic assumptions of the present model are: (a) in the absence of apical Na^+, the overall tissue electrical conductance (G) mainly reflects the conductance of the extracellular route (Castro et al., 1993; Lacaz-

Vieira and Kachar, 1996). (b) The TJ is the main barrier of the extracellular route. (c) The degree of TJ permeability is controlled by the extracellular Ca^{2+} concentration at the zonula adhaerens, where Ca^{2+} binding sites that control the formation and maintenance of the junctional complex are located (Gumbiner et al., 1988).

To test the model adequacy in describing the experimental results, results obtained in different experimental conditions will be compared with forecasts generated by modeling in equivalent situations. Conceivable inconsistencies might be found, indicating that a further refinement of the model is needed. Our initial aim is to describe the observed experimental results in a semiquantitative way, which means that we are not pursuing exact numerical values matching the observed experimental responses (for a lack of access to all relevant parameters that characterize the system), but to get a mathematical simulation that closely resembles the time course of the observed experimental results.

Studies on the fine structure of amphibian urinary bladders (Pak Poy and Bentley, 1960; Peachey and Rasmussen, 1961; Choi, 1963) show that the overall thickness of the bladder wall is ~100 μm, the epithelium comprising nearly 10% of this value and the rest consisting basically of the submucosa, since the serosal layer is extremely flat. These dimensions vary among preparations and as a result of the degree of stretching the bladder is submitted to when mounting. So, care was taken to inflate the bladders, as much as possible, in the same way before gluing the tissue to the supporting plastic ring (see MATERIALS AND METHODS).

The diagram of Fig. 1 A is a schematic representation of the frog urinary bladder showing its major structures, with particular emphasis on the extracellular route (ER). To our modeling purpose, the extracellular route is an aqueous pathway that communicates the apical solution with the basal solution. It can be conceived of as an unstirred aqueous compartment which comprises the paracellular space between the epithelial cells in series with the extracellular fluid of the submucosa (submucosal fluid). In addition to it we have to add the contribution of an unstirred layer on the surface of the tissue (Levine et al., 1984).

The ER was modeled as a continuous aqueous medium (Fig. 1 B) connecting the apical solution to the basal solution and the TJ as a controlled barrier located at the apical end of ER. The basal end of ER is open to the basal solution. For computation purpose, ER was approximated as a linear array of cells (0, 1, 2, ... N) (Fig. 1 C). Cell 0 is the most apical one and is separated from the apical solution by the TJ. The last cell (cell N) is the most basal one and is directly in contact with the basal solution. All cells are identical in size.

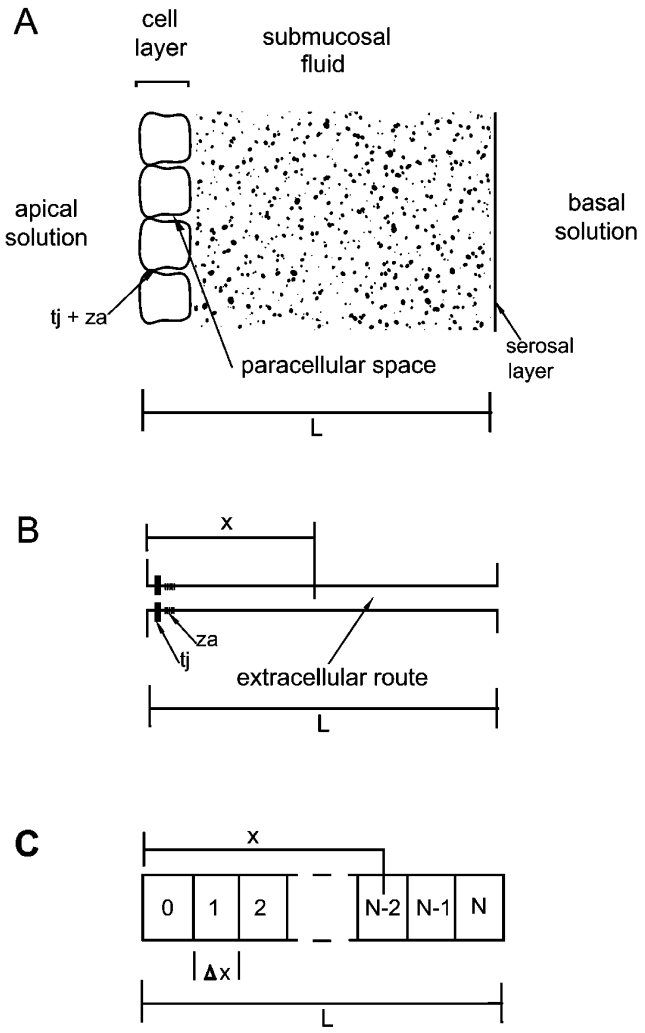

FIGURE 1. (A) Diagram of a transversal section through a frog urinary bladder showing (out of scale) the epithelial layer having a thickness of ~10 μm and the submucosa that consists of a delicate stroma of fibroblasts and collagen fibers, blood and lymph vessels, nerves, and smooth muscle bundles embedded in the submucosal fluid, with a total thickness of ~100 μm. (B) Simplified schematic representation of the extracellular route which comprises the paracellular space in series with the submucosal fluid. The extracellular route is presented as an aqueous unstirred compartment having one end in contact with the apical solution and the other with the basal solution. The tight junction (TJ) is represented as a gate which controls access to the apical opening of the extracellular route. Near the TJ are depicted the Ca^{2+} binding sites of the zonula adhaerens (za). (C) Modeling of diagram B as a linear array of cells (0, 1, 2, ... N).

Cell 0 corresponds to the microenvironment of zonula adhaerens where the Ca^{2+} binding sites which control the formation and maintenance of epithelial junctional complex (Gumbiner et al., 1988) are located. $Ca^{2+}{}_0$ is determined by the rate of Ca^{2+} diffusion across the TJ and the rate of Ca^{2+} diffusion across the boundary between cell 0 and 1. Thus, $Ca^{2+}{}_0$ is affected, among other variables, by the Ca^{2+} concentrations in

the bathing solutions, Ca^{2+}_{ap} and Ca^{2+}_{bl}. The apical Ca^{2+} concentration may affect Ca^{2+}_0 only when the TJ is permeable and Ca^{2+} can move across the TJ depending on the difference $(Ca^{2+}_{ap} - Ca^{2+}_0)$. In addition, Ca^{2+}_0 is affected by changes in Ca^{2+}_{bl} since Ca^{2+} can diffuse along the extracellular route depending on $(Ca^{2+}_{bl} - Ca^{2+}_0)$. Changes in Ca^{2+}_{bl} are expected to induce changes in the concentration profile along the extracellular route $Ca^{2+}_{er}(N, t)$ according the Fick's second law (Crank, 1956; Sten-Knudsen, 1978). The Ca^{2+} concentration profile along the extracellular route adjusts itself to a new profile when Ca^{2+}_{bl} is altered. With the TJ closed and in a steady-state condition Ca^{2+}_0 is expected to be equal to Ca^{2+}_{bl}.

The model just presented is described by the following system of partial differential equations (Crank, 1956; Sten-Knudsen, 1978).

For $x = 0$:

$$\frac{\partial Ca_{er}^{++}(0, t)}{\partial t} = K_{TJ}(t, Ca_{er}^{++}[0, t])(Ca_{ap}^{++}[t] - Ca_{er}^{++}[0, t]) + D\frac{\partial Ca_{er}^{++}(0, t)}{\partial x}, \quad (1)$$

with

$$K_{TJ}(t, Ca_{er}^{++}[0, t]) = K\ G(t - \theta, Ca_{er}^{++}[0, t - \theta]) \quad (2)$$

$$G(\tau, Ca_{er}^{++}[0, \tau]) = \frac{1}{1 + \dfrac{R_0}{1 + (K_m / Ca_{er}^{++}[0, \tau])^n}}. \quad (3)$$

For $0 < x < L$:

$$\frac{\partial^2 Ca_{er}^{++}(x, t)}{\partial x^2} = -D\left(\frac{\partial Ca_{er}^{++}[x, t]}{\partial t}\right), \quad (4)$$

subject to

$$Ca_{er}^{++}(L, t) = Ca_{bl}^{++}(t) \quad (5)$$

$D = Ca^{2+}$ diffusion coefficient in water, equal to $0.79 \times 10^{-5}\ cm^{-2}\ s^{-1}$ (Hille, 1992).

Discretized model

The partial differential Eqs. 1–5 can be approximated by a system of ordinary differential equations, discretizing the total length L into a series of N finite elements of length Δx such that $\Delta x = L/N$. The obtained approximated model, presented below, can be easily implemented on a computer.

For $x = 0$:

$$\frac{\partial Ca_{er}^{++}(0, t)}{\partial t} = K_{TJ}(t, Ca_{er}^{++}[0, t])(Ca_{ap}^{++}[t] - Ca_{er}^{++}[0, t]) + \frac{D}{\Delta x}(Ca_{er}^{++}[\Delta x, t] - Ca_{er}^{++}[0, t]) \quad (6)$$

For $x = k\Delta x$, $k = 1, 2, 3...N$:

$$-D\frac{\partial Ca_{er}^{++}(x, t)}{\partial t} = \frac{Ca_{er}^{++}(x + \Delta x, t) - 2Ca_{er}^{++}(x, t) + Ca_{er}^{++}(x - \Delta x, t)}{\Delta x^2} \quad (7)$$

For $x = L$

$$-D\frac{\partial Ca_{er}^{++}(L, t)}{\partial t} = \frac{Ca_{bl}^{++}(t) - 2Ca_{er}^{++}(L, t) + Ca_{er}^{++}(L - \Delta x, t)}{\Delta x^2} \quad (8)$$

For the sake of numerical integration of the diffusion equation, N was considered equal to 100.

The model main components depicted in Fig. 2 A are: (a) the Ca^{2+} binding sites of zonula adhaerens (the sensor), (b) the cell machinery involved in the cell signaling process (control unit), and (c) the TJ barrier which is the effector. The sensor transduces the Ca^{2+} concentration level in cell 0 and sends information to the control unit which responds with an output signal that modulates the permeability of the TJ barrier (the effector). The apical and basal solutions are well stirred and their composition, particularly the Ca^{2+} concentration, properly adjusted. Fig. 2 B shows a block diagram that is a pictorial represen-

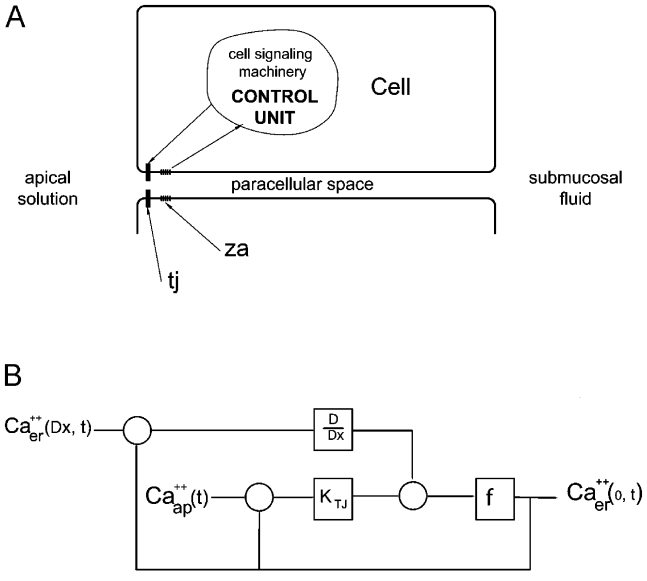

FIGURE 2. (A) Schematic representation of the feedback loop involved in the control of the tight junction barrier with its main components: (a) the sensor is the Ca^{2+} binding sites of *zonula adhaerens* (za); (b) the control unit is the cell machinery involved in the cell signaling process; and (c) the effector is the TJ barrier. The black arrows indicate the direction of information flow from za to the TJ. (B) Block diagram representing the function of each component of the feedback loop shown in (A) as well as the flow of signals. See RESULTS, The Model, for explanation.

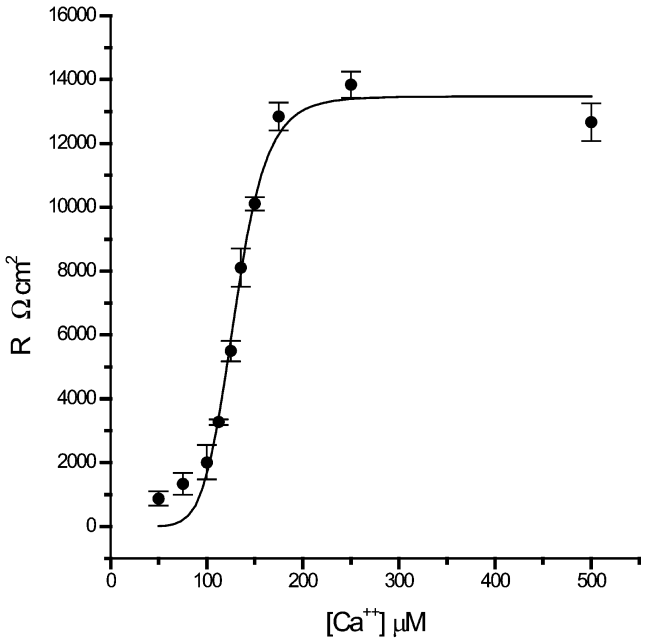

FIGURE 3. Mean steady-state values for transepithelial electrical resistance (R) as a function of Ca^{2+} concentration in both apical and basal bathing solutions for 4 different frog urinary bladder preparations. The basal solution was NaCl-Ringer's and the apical solution KCl 75 mM with the same Ca^{2+} concentration as that of the basal solution. Na^+ was removed from the apical solution in order to reduce the contribution of transcellular electrical conductance to the overall tissue electrical conductance. Data points were fitted according to the Hill equation (Eq. 9) (see RESULTS, The Model).

tation (according to the conventions of control engineering [Ogata, 1998]) of the functions performed by each component of the system, as well as the flow of signals.

The degree of TJ sealing was assumed to depend on the Ca^{2+} concentration at the Ca^{2+} binding sites of zonula adhaerens ($Ca^{2+}{}_0$) (Gumbiner et al., 1988). In physiological conditions $Ca^{2+}{}_0$ is around 1 mM (equal to $Ca^{2+}{}_{bl}$), which maintains the TJs closed. Lowering $Ca^{2+}{}_{bl}$ causes a decline of $Ca^{2+}{}_0$ that, reaching a certain critical value (~0.1–0.5 mM depending on the preparation), triggers TJ opening. In a steady-state condition, within a certain range of $Ca^{2+}{}_0$ values, a relationship holds between $Ca^{2+}{}_0$ and the degree of opening of the TJ barrier, as evaluated by the tissue electrical resistance (Fig. 3), which is in agreement with previous studies (Jovov et al., 1994; Lacaz-Vieira, 1997). In the present model, this dependence is expressed by Eq. 2.

K_{TJ} as a Function of $Ca^{2+}{}_0$

The main barrier of ER is the TJ. Therefore, the electrical resistance of ER is mainly determined by the TJ. Consequently, we can assume in a first approximation that the permeability of the TJs, expressed by $K_{TJ}(t,Ca^{2+}{}_{er}(0, t))$, and tissue electrical conductance ($G = 1/R$) are linearly related (Byrne and Schultz, 1988; Schultz, 1980).

The function that expresses the relationship between $K_{TJ}(t,Ca^{2+}{}_{er}[0, t])$ and $Ca^{2+}{}_{er}(0, t)$ was tentatively chosen according to (Jovov et al., 1994; Lacaz-Vieira, 1997) and to the experimental data presented in Fig. 3, where steady-state tissue electrical resistance (R) is plotted against the Ca^{2+} concentration in the external bathing solutions (apical and basal solutions), which should be equal to $Ca^{2+}{}_{er}(0, t)$. As can be seen, the dependence of R on $Ca^{2+}{}_{er}(0, t)$ is sigmoidal and well fitted by the Hill equation as proposed previously for A6 cell monolayers (Jovov et al., 1994) and frog urinary bladder (Lacaz-Vieira, 1997). As seen, R is very large for $Ca^{2+}{}_{er}(0, t)$ above a critical value, and decreases rapidly for $Ca^{2+}{}_{er}(0, t)$ values below this critical value (Fig. 3). According to the Hill equation:

$$R = R_0/(1 + [K_m/Ca^{++}{}_0]^n) \quad (9)$$

For computation purposes, a modification of the Hill equation was made by introducing an additive term, A, so as to limit the value of R to a minimum, different from zero, when $Ca^{2+}{}_0$ is made equal to zero, as when $Ca^{2+}{}_{bl}$ is removed in the absence of $Ca^{2+}{}_{ap}$.

Thus:

$$R = \{R_0/(1 + [K_m/Ca^{++}{}_0]^n)\} + A \quad (10)$$

As $G = 1/R$ then:

$$G = (1/\{R_0/(1 + [K_m/Ca^{++}{}_0]^n)\} + A). \quad (11)$$

Steady-state Transepithelial Electrical Resistance Values (R) as a Function of Equal Ca^{2+} Concentration in both Apical and Basal Bathing Solutions

These experiments were performed to determine R steady-state values as a function of the Ca^{2+} concentration at zonula adhaerens ($Ca^{2+}{}_0$). To accomplish this condition, $Ca^{2+}{}_{ap}$ and $Ca^{2+}{}_{bl}$ were made the same. Under this condition $Ca^{2+}{}_0$ is expected to be identical to that in the bathing solutions. As observed in Fig. 3 for steady-state condition (for 4 different urinary bladders) R is a sigmoidal function of Ca^{2+} concentration in the bathing solutions and adequately fitted by the Hill equation (Eq. 9) (see RESULTS, The Model) (Jovov et al., 1994; Lacaz-Vieira, 1997). Calculated parameters from the fitting of the experimental data are as follows: $R_o = 13472.5 \pm 488.9\ \Omega\ cm^2$; $K_m = 0.1293 \pm 0.0025$ mM and $n = 7.8 \pm 1.1$.

TJs Remain Closed When Normal Ca^{2+} Concentration Is Present in the Bathing Solutions

When NaCl-Ringer's solution (Ca^{2+} 1 mM) is present on both apical and basal sides of the bladder (thus $Ca^{2+}{}_{ap} = Ca^{2+}{}_{bl} = 1$ mM) the TJs remain closed. This is characterized by G staying stable at its lowest value (Fig.

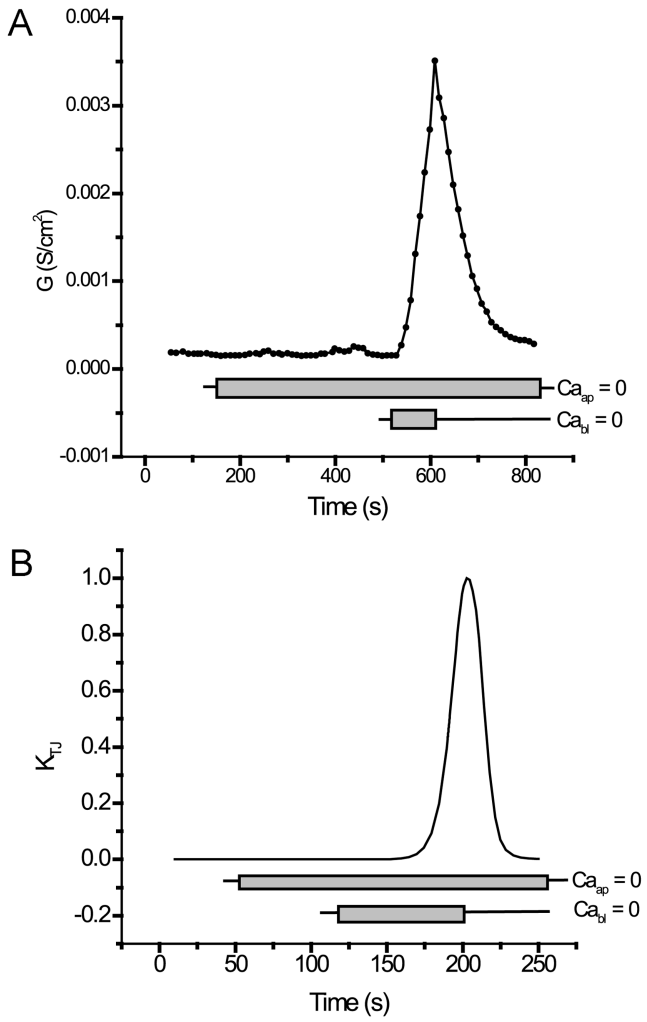

FIGURE 4. (A) Representative experiment of an FCSA performed in a fragment of frog urinary bladder. At the start of the experiment, tissue was bathed on the apical side by KCl 75 mM containing 1 mM Ca^{2+} and on the basal side by NaCl-Ringer's solution. Then, 100 s after the beginning of the record, Ca^{2+} was removed from the apical solution and no effect was observed on G. Finally, Ca^{2+} was removed from the basal solution and subsequently reintroduced according to the protocol of an FCSA. As observed, G increases when $Ca^{2+}_{bl} = 0$ mM and recovers when $Ca^{2+}_{bl} = 1$ mM. (B) Model prediction for G in response to apical Ca^{2+} removal followed by a simulation of a FCSA which consists of Ca^{2+} removal and subsequent addition to the basal solution. Parameters and variables: dx = 3 μm; K = 1.5 s^{-1}; θ = 5 s; $Ca^{2+}_{ap} = 1$ mM (t = 0 s); $Ca^{2+}_{ap} = 0$ mM (t = 50 s); $Ca^{2+}_{bl} = 0$ mM (t = 120 s); $Ca^{2+}_{bl} = 1$ mM (t = 190 s). K_{TJ} is normalized to its maximum value.

4 A). The model predicts these behaviors since K_{TJ} remains stable at its lowest predicted value (Fig. 4 B).

Ca^{2+} Removal from the Apical Solution Does Not Lead to TJ Opening

These experiments were performed by removing Ca^{2+} from the apical solution (thus $Ca^{2+}_{ap} = 0$ mM and $Ca^{2+}_{bl} = 1$ mM). As observed experimentally, Ca^{2+} removal from the apical solution does not alter G, indicating that the TJs remain closed (Fig. 4 A). The model predicts this behavior since K_{TJ} remain stable at its lowest value (Fig. 4 B).

Basal Ca^{2+} Removal in the Absence of Apical Ca^{2+} Leads to TJ Opening and Return of Ca^{2+} Induces TJ Closing

These experiments were performed according to the FCSA protocol (see MATERIALS AND METHODS). When Ca^{2+}_{bl} is removed, the TJs start to open after a variable delay (generally between 30 s and 3 min; mean value 103.0 ± 9.2 s [n = 22] [Lacaz-Vieira, 2000]). This response is characterized by a progressive increase of G. Return of Ca^{2+} to the basal solutions causes a halt in the process of junction opening and recovery taking place, leading ultimately to a complete closure of the TJ seal, G achieving the initial control value (Fig. 4 A). This response has been described previously (Lacaz-Vieira, 1997, 2000) and interpreted as resulting from drop of Ca^{2+}_0 due to Ca^{2+} diffusing along the ER according to its concentration gradient. When a critical Ca^{2+}_0 level is reached a signal is triggered, leading to the opening of the TJs. If Ca^{2+} is not reintroduced into the basal fluid the TJs continue to open, followed ultimately by cell detachment. However, in all our experiments this unwanted happening was prevented as TJ opening is always halted (when G reached values of the order of 5×10^{-3} S) by the reintroduction of Ca^{2+}_{bl}; avoiding, therefore, more complex regulatory responses such as endocytosis, cytoskeleton changes, and protein phosphorylation and further cell detachment. Our model predicts the observed time course behavior, including the delay between Ca^{2+} removal and the start of junction opening (Fig. 4 B).

So that the simulation results closely match the average experimental responses to a FCSA, dx = 3 μm was used in the calculations. This would indicate that the total diffusion length (ER plus the thickness of the unstirred layer adjacent on the basal surface of the tissue, including a tortuosity factor along ER) would be equivalent to 300 μm. The contribution of a significant unstirred layer adjacent to the surface of the tissue is supported by experimental data of Levine et al. (1984) obtained in toad urinary bladder where unstirred layers of the order of 46 μm were detected in high-speed steering chambers (Levine et al., 1984) that perform a much more vigorous steering than the chambers used in the present study. For the Hill equation (Eq. 3) we used $R_o = 13472.5 \pm 488.9\ \Omega\ cm^2$; and $n = 7.8 \pm 1.1$ as calculated from the results of Fig. 3. However, a $K_m = 0.1293 \pm 0.0025$ mM, as calculated from data of Fig. 3, did not allow an adequate fitting. By trial and error we found that increasing K_m would favor a better fitting. (Although it is difficult to justify this adjustment from

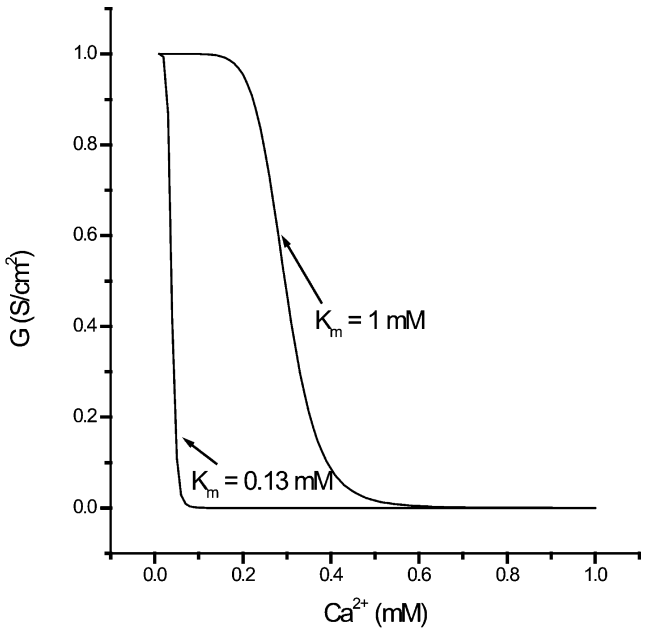

FIGURE 5. Tissue steady-state electrical conductance (G) as a function of the Ca^{2+} concentration in the bathing solutions. Curve on the left was generated using the parameters calculated from data of Fig. 3. Curve on the right was generated using the same parameters except K_m that was increased to 1 mM.

first principles, it appears to be valid on the grounds of a good matching between the predicted behavior and the experimental results as observed throughout this study.) A value of ~1 mM was found adequate. This is significantly larger than the steady-state experimentally obtained value. However, we have to consider that the results presented in Fig. 3 are steady-state values and the FCSA responses are transient phenomena which could not necessarily be adequately simulated using steady-state parameters. To better understand this discrepancy, curves depicting G as a function of Ca^{2+} concentration in the bathing solutions were generated, using the steady-state parameters obtained from Fig. 3 (R_o = 13472.5 ± 488.9 Ω cm²; K_m = 0.1293 ± 0.0025 mM and n = 7.8 ± 1.1) and with K_m = 1 mM (Fig. 5). As can be seen with K_m = 0.1293 mM, the curve is markedly shifted to the left. In contrast, with K_m = 1 mM the curve that depicts the dependence of G on $Ca^{2+}{}_0$ is situated in a region more consistent with the observed dynamic behavior.

According to the model, the delay that is observed between $Ca^{2+}{}_{bl}$ removal and TJ opening results from two different components. One is the Ca^{2+} diffusion delay along the unstirred aqueous region (paracellular space, submucosal fluid and the unstirred layer) when $Ca^{2+}{}_{bl}$ is changed. The other is the delay in cell signaling, the time information takes to go from the Ca^{2+} binding sites of zonula adhaerens to the onset of molecular TJ alterations that result in G alteration. Increasing the diffusion thickness (Δx) not only causes an increase in the delay of TJ opening, but has a marked effect upon time course of TJ closing that becomes slower. This explains why large differences in delays and time courses of FCSA responses are experimentally observed.

Apical Ca^{2+} Significantly Affects the Time Course of TJ Opening during a FCSA, Depending on its Concentration and Instant of Application

The rate of TJ opening, evaluated by the rate of G increase in an FCSA, is reduced when Ca^{2+} is present in the apical solution. A high $Ca^{2+}{}_{ap}$ may even keep the TJs insensitive to a Ca^{2+}-free basal solution (Lacaz-Vieira, 1997), the TJs remaining closed for long periods of time.

Introduction of apical Ca^{2+} during the process of TJ opening in an FCSA may slow down TJ opening when a low apical Ca^{2+} concentration is used. Stop of TJ opening followed by partial recovery and subsequent attainment of a new G steady-state can be observed for higher (~1 mM) apical Ca^{2+} concentrations. Frequently, oscillations of TJ permeability, characterized by oscillations of G, are observed when TJ opening is induced by an FCSA and Ca^{2+} is added to or is already present in the apical solution. The kind of response is determined by the $Ca^{2+}{}_{ap}$ concentration and by differences among tissues. When different epithelia are tested responses can be quite distinct. Thus, oscillations are clearly observed in the great majority of frog urinary bladders (Lacaz-Vieira, 2000), but were never seen in A6 cell monolayers (Lacaz-Vieira et al., 1999; Lacaz-Vieira and Jaeger, 2001). The model we are presenting predicts all the observed response patterns, depending on an adequate adjustment of its parameters.

An example of $Ca^{2+}{}_{ap}$ inducing a stop of TJ opening and partial recovery reaching a new G steady-state without oscillations is shown in Fig. 6 A. The model prediction of this behavior is presented in Fig. 6 B. This kind of response, showing a partial recovery followed by an escape phase in which G increases again toward a new steady-state, has been described previously (Lacaz-Vieira, 2000). Absence of oscillations can be modeled by reducing the value of the parameter θ (the delay in cell signaling). The escape phase is not always observed as depicted in Fig. 7, A and B. Comparison of Figs. 6 B and 7 B show that a small change of $Ca^{2+}{}_{ap}$ concentration can drastically affect the pattern of the response as, for example, the presence or absence of the escape phase.

Oscillations of G, reflecting TJ permeability oscillations, are frequently observed during the phase that the TJs are opening in an FCSA and Ca^{2+} is added to the apical fluid (Fig. 8 A), or when Ca^{2+} is already present in the apical fluid when the FCSA is started

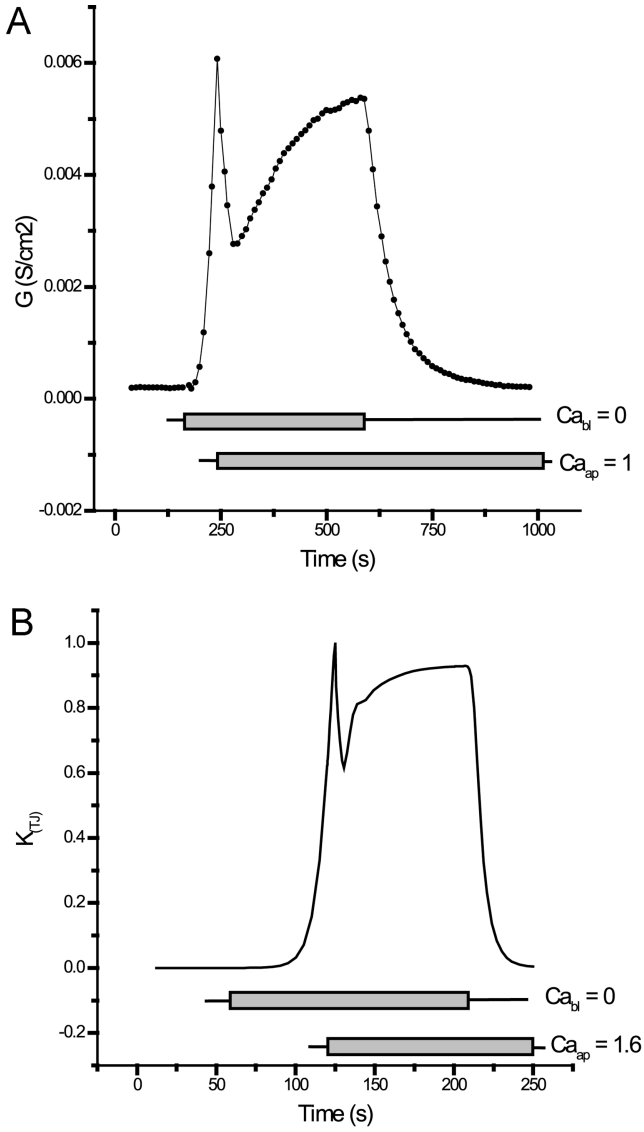

FIGURE 6. (A) Representative experiment on the effect of apical Ca^{2+} addition on the response to an FCSA. Effect of adding Ca^{2+} to the apical bathing solution at 1 mM concentration after G had increased in response to Ca^{2+}_{bl} removal. In this case, the presence of apical Ca^{2+} induced a halt in the process of TJ opening followed by partial recuperation of G, which is then accompanied by a escape phase, characterized by a later increase of G toward a new steady-state. (B) Model prediction for G in response to apical Ca^{2+} addition. Parameters and variables: dx = 3 μm; K = 1.07 s^{-1}; θ = 5 s; Ca^{2+}_{bl} = 0 mM (t = 50 s); Ca^{2+}_{ap} =1.6 mM (t = 120 s); Ca^{2+}_{bl} = 1 mM (t = 200 s). K_{TJ} is normalized to its maximum value.

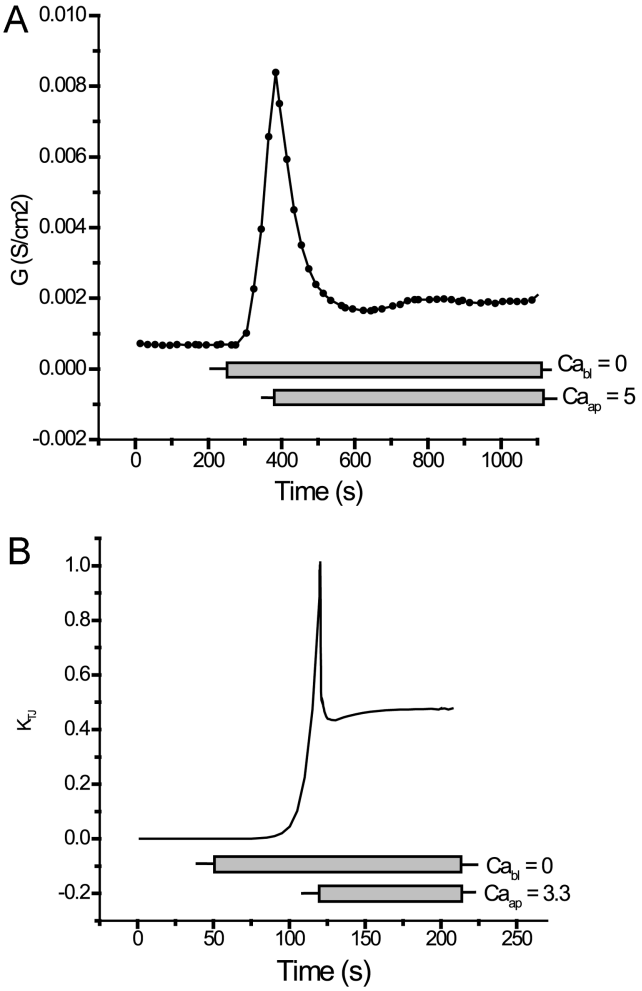

FIGURE 7. (A) Representative experiment on the effect of apical Ca^{2+} addition on the response to an FCSA. Effect of adding Ca^{2+} to the apical bathing solution at 5 mM concentration after G had increased in response to Ca^{2+}_{bl} removal. In this case, the presence of apical Ca^{2+} induced a halt in the process of TJ opening followed by partial recuperation of G which stabilize in a new steady-state. (B) Model prediction for G in response to apical Ca^{2+} addition. Parameters and variables: dx = 3 μm; K = 1 s^{-1} ; θ = 0.5 s; Ca^{2+}_{bl} = 0 mM (t = 50 s); Ca^{2+}_{ap} = 3.3 mM (t = 120 s). K_{TJ} is normalized to its maximum value.

(Fig. 9 A). Simulations of these experimental conditions are shown in Figs. 8 B and 9 B, respectively. One of the conditions for oscillations to occur, in addition to the topological organization of the Ca^{2+} binding sites being located in the paracellular space, just basal to the TJs (which sets up the conditions for the existence of a closed feedback loop), is the existence of an information delay (θ) between the signal starting at the Ca^{2+} binding sites and the TJ response. The model never oscillates for θ = 0. For example, regarding Fig. 8 B, a progressive reduction of θ from 5 to lower values gives rise to progressively more dumped oscillations (unpublished data) up to θ = 0.5, when oscillations totally vanish. When Ca^{2+} is already present in the apical solution and an FCSA is triggered, oscillations start with a variable delay (seconds to a few minutes) after Ca^{2+}_{bl} is removed (Fig. 9, A and B) and the amplitude of oscillations initially increase with time. In contrast, when the concentration of Ca^{2+}_{ap} is high (10–50 mM) the removal of Ca^{2+}_{bl} (FCSA) causes only a small increase of G and this situation may remain stable. Later, if Ca^{2+}_{ap} is removed then a sharp increase of G with a

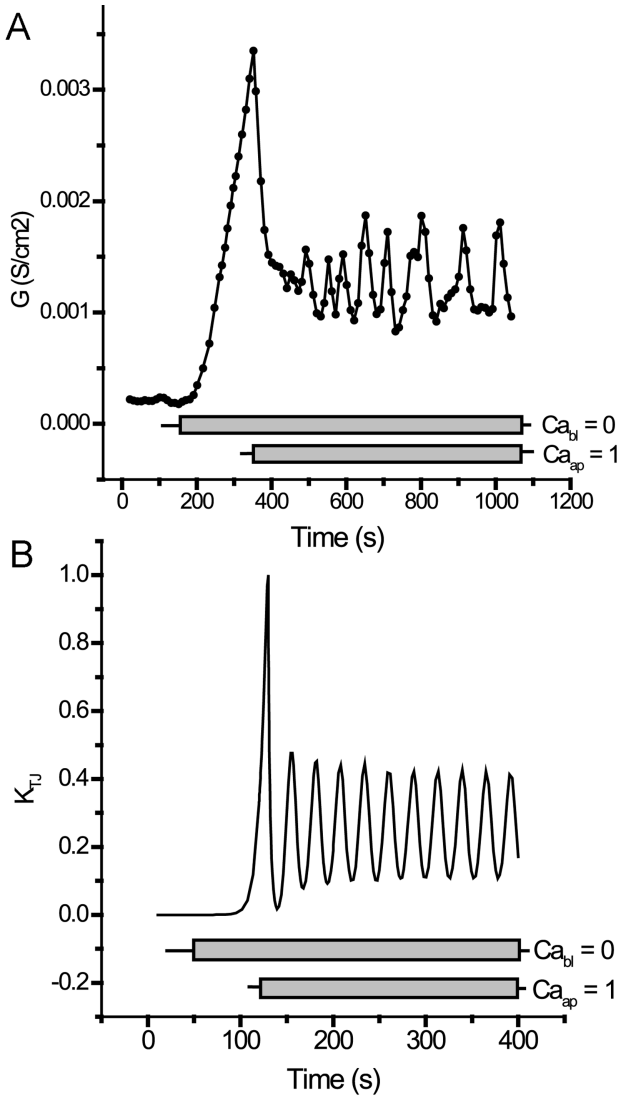

FIGURE 8. (A) Representative experiment on the effect of apical Ca^{2+} addition on the response to an FCSA. Effect of adding Ca^{2+} to the apical bathing solution at 1 mM concentration after G had increased in response to Ca^{2+}_{bl} removal. In this case, the presence of apical Ca^{2+} induced a halt in the process of TJ opening followed by partial recuperation of G that is accompanied by oscillations of G. (B) Model prediction for G in response to apical Ca^{2+} addition. Parameters and variables: dx = 3 μm; K = 8 s^{-1}; θ = 10 s; Ca^{2+}_{bl} = 0 mM (t = 50 s); Ca^{2+}_{ap} = 1 mM (t = 120 s). K_{TJ} is normalized to its maximum value.

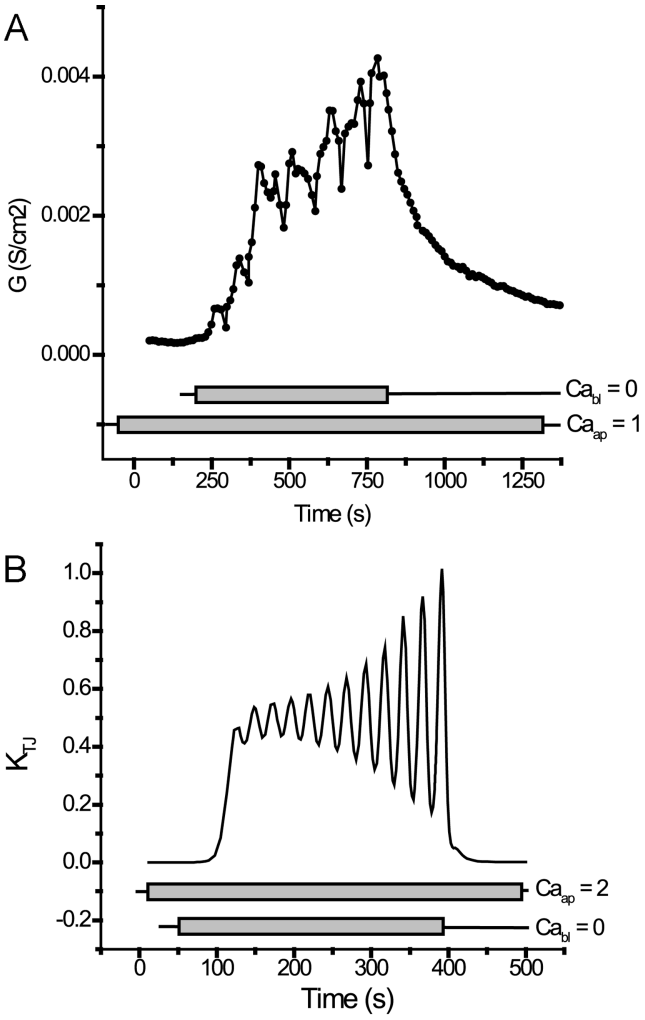

FIGURE 9. (A) Representative experiment on the effect of the previous presence of apical Ca^{2+} on the time course of G increase in response to an FCSA. Ca^{2+}_{ap} was already present at 1 mM concentration when the FCSA was induced by removing Ca^{2+}_{bl}. In this case, due to the presence of apical Ca^{2+}, the FCSA induced oscillations which started soon after Ca^{2+}_{bl} was removed. These oscillations increased in amplitude until a steady-state is reached. (B) Model prediction for G in response to Ca^{2+}_{bl} removal. Parameters and variables: dx = 3 μm; K = 5 s^{-1}; θ = 9.25 s; Ca^{2+}_{ap} = 2 mM (t = 0 s); Ca^{2+}_{bl} = 0 mM (t = 50 s); Ca^{2+}_{bl} = 1 mM (t = 382 s). K_{TJ} is normalized to its maximum value.

very short delay (as compared with the normal FCSA) is observed (Fig. 10 A). This behavior is clearly simulated by the model we are proposing (Fig. 10 B).

DISCUSSION

The current simulation of the dynamical behavior of TJs of the frog urinary bladder in response to alterations in the Ca^{2+} concentration in the bathing solutions originated from the aim to validate a previous interpretation (Lacaz-Vieira, 2000) that oscillations of tissue electrical conductance (G) result from oscillations of TJ permeability due to a negative feedback loop that sets up when the TJ seal is opened by removal of Ca^{2+}_{bl} and Ca^{2+} is present in the apical bathing fluid.

The present modeling allows us to understand and reproduce all major aspects of the dynamic behavior of TJs such as: (a) the TJs remain closed when normal Ca^{2+} concentration is present in the bathing solutions; (b) Ca^{2+}_{ap} removal does not lead to TJ opening; (c) Ca^{2+}_{bl} removal in the absence of Ca^{2+}_{ap} leads to TJ opening after a significant delay and return of Ca^{2+}_{bl} induced the closing of the TJs, in a procedure know as

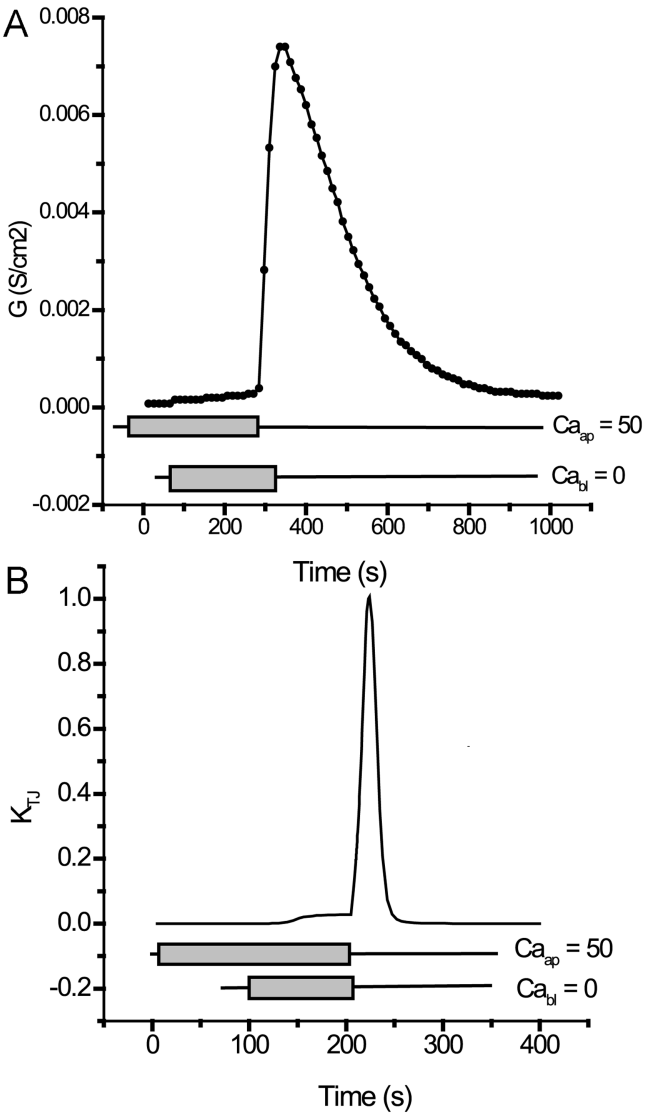

FIGURE 10. (A) Representative experiment on the effect of the previous presence of apical Ca^{2+} at high concentration on the time course of G increase in response to an FCSA. Ca^{2+}_{ap} was already present at 50 mM concentration. Ca^{2+}_{bl} removal caused a small increase in conductance. Afterwards, Ca^{2+}_{ap} was removed inducing a fast rising increase of G, with a short latency period. Soon after, Ca^{2+}_{bl} was raised to 1 mM, causing a recovery of the TJ seal. (B) Model prediction for G in response to to a situation equivalent to that in A. Parameters and variables: dx = 3 μm; K = 1.5 s^{-1}; θ = 5 s; Ca^{2+}_{ap} = 50 mM (t = 0 s); Ca^{2+}_{bl} = 0 mM (t = 100 s); Ca^{2+}_{ap} = 0 (t = 200); Ca^{2+}_{bl} = 1 (t = 210). K_{TJ} is normalized to its maximum value.

FCSA; (d) the presence of Ca^{2+}_{ap} significantly affects the time course of TJ opening in a FCSA depending on its concentration and the moment of application; (e) a high concentration of Ca^{2+}_{ap} may even render the TJs insensitive to Ca^{2+}_{bl} removal; (f) addition of Ca^{2+}_{ap} in the course of TJ opening in a FCSA may slow down the process of junction opening or cause partial recuperation of the TJ seal followed by a escape phase, depending on its concentration; and (g) frequently, oscillations of TJ permeability are observed when Ca^{2+} is added to the apical solution in the course of junction opening phase of a FCSA.

The operation of the feedback loop allows us to understand the above responses. Thus, a sudden rise of Ca^{2+}_{ap} when the TJs are opening causes Ca^{2+} diffusion through the TJs, increasing Ca^{2+} concentration at the Ca^{2+} binding sites of zonula adhaerens, triggering a regulatory TJ closing, characterized by a sharp drop of G. This in turn limits diffusion of Ca^{2+} from the apical solution to the zonula adhaerens. The basal solution, where Ca^{2+}_{bl} = 0 mM during the TJ opening phase of the FCSA, behaves as a Ca^{2+} sink allowing Ca^{2+} to diffuse from the zonula adhaerens region, along the extracellular route, into the solution, leading to a drop of the Ca^{2+} concentration at the Ca^{2+} binding sites of zonula adhaerens, and causing stabilization of the Ca^{2+} concentration in this region at an intermediate value between those in the apical and the basal compartments, respectively. Consequently, the TJ permeability adjusts to a new value according to the Hill equation (see RESULTS, The Model). Frequently, the presence of Ca^{2+}_{ap} during TJ opening in an FCSA leads to G oscillations of low frequency. Oscillations of TJ permeability were interpreted (Lacaz-Vieira, 2000) as resulting from the operation of a negative feedback loop since the effector, the TJ barrier, limits the access of the control signal (Ca^{2+} originating from the apical solution) to its site of action (the Ca^{2+} sites of E-cadherin in the zonula adhaerens). Under certain conditions, the corrective action in a feedback loop can produce unstable operation and the system may drive to limiting values or show oscillations (Weyrick, 1975; Ogata, 1998). Time delays or lags in the response are normally the cause of instability or oscillations. Inherent time delays may prevent the stopping of the control action in time to avoid overshoot of the controlled variable, which, in turn, may result in a corrective action in the opposite direction. This may cause the feedback to reinforce rather than oppose the input signal, resulting in continuous or damped oscillations. The theory of automatic controls shows that accuracy and stability are mutually incompatible (Weyrick, 1975). Accuracy is improved as loop gain is increased. However, increase in gain also tends to make the system unstable. The delay θ (the cell signaling delay) is particularly important for oscillations to occur since oscillations cannot be observed when θ = 0 or close to it.

The delay of TJ opening after Ca^{2+}_{bl} is removed results of basically two different lags. One is a diffusion delay along the unstirred aqueous compartment of the extracellular route. The other from the time information takes to travel from the sensor region (Ca^{2+} biding sites) to the effector (the TJ). The combination of

these may explain why different delays are normally observed. Some tissues respond to a FCSA in <1 min, others take >3 min to start TJ opening.

The frequency of oscillations may differ when different bladder preparations are compared. This is a reasonable occurrence since, according to model predictions, changes in parameter values may importantly alter the oscillatory behavior, even determining their existence or absence. When a given tissue is tested, we can observe experimentally that a decrease of $Ca^{2+}{}_{ap}$ from 5 to 1 mM leads to a 21.7% increase of the oscillation frequency from a values of 0.011 Hz obtained with $Ca^{2+}{}_{ap}$ = 5 mM (n = 5). In agreement with it, the model also predicts an increase of frequency with a decrease of $Ca^{2+}{}_{ap}$. Thus, for K = 5 s^{-1} and θ = 5 s, a progressive decrease of $Ca^{2+}{}_{ap}$ from 10 to 5 and to 2.4 mM increases the frequency of oscillation respectively from 0.062 to 0.068 and to 0.080 s^{-1}.

The analysis of oscillations—their amplitude, frequency, occurrence, and response to drugs—might allow us to probe and understand better the control system that regulate TJ opening and closing. Thus, inhibition of PKC by H7 causes a prompt stop of TJ oscillations, which reappear when the inhibitor is removed (Lacaz-Vieira, 2000). This effect can be thought as resulting from a block by H7 of the information loop that connects the Ca^{2+} sites of zonula adhaerens (the sensor) to the TJs (the effector).

Supported by grants from Fundação de Amparo à Pesquisa do Estado de São Paulo (FAPESP) (99/03077-5) and Conselho Nacional de Desenvolvimento Científico e Tecnológico (CNPq) (303633/85-9).

Submitted: 2 April 2002
Revised: 12 June 2002
Accepted: 14 June 2002

REFERENCES

Balda, M.S., M.B. Fallon, C.M. Van Itallie, and J.M. Anderson. 1992. Structure, regulation, and pathophysiology of tight junctions in the gastrointestinal tract. *Yale J. Biol. Med.* 65:725–735.

Byrne, J.H., and S.G. Schultz. 1988. An Introduction to Membrane Transport and Bioelectricity. Raven Press, New York. 1–232.

Castro, J.A., A. Sesso, and F. Lacaz-Vieira. 1993. Deposition of BaSO4 in the tight junctions of amphibian epithelia causes their opening; apical Ca2+ reverses this effect. *J. Membr. Biol.* 134:15–29.

Cereijido, M., L. González-Mariscal, G. Avila, and R.G. Contreras. 1988. Tight junctions. *CRC Crit. Rev. Anat. Sci.* 1:171–192.

Cereijido, M., L. Shoshani, and R.G. Contreras. 2000. Molecular physiology and pathophysiology of tight junctions. I. Biogenesis of tight junctions and epithelial polarity. *Am. J. Physiol. Gastrointest. Liver Physiol.* 279:G477–G482.

Choi, J.K. 1963. The fine structure of the urinary bladder of the toad bufo marinus. *J. Cell Biol.* 16:53–72.

Crank, J. 1956. The Mathematics of Diffusion. Oxford University Press, NY. 414 pp.

Gumbiner, B., B.R. Stevenson, and A. Grimaldi. 1988. The role of the cell adhesion molecule uvomorulin in the formation and maintenance of epithelial junctional complex. *J. Cell Biol.* 107: 1575–1587.

Hille, B. 1992. Ionic Channels of Excitable Membranes. Sinauer Associates, Inc., Sunderland, MA. 607 pp.

Hopkins, A.M., D. Li, R.J. Mrsny, S.V. Walsh, and A. Nusrat. 2000. Modulation of tight junction function by G protein-coupled events. *Adv. Drug Deliv. Rev.* 41:329–340.

Jovov, B., S.A. Lewis, W.E. Crowe, J.R. Berg, and N.K. Wills. 1994. Role of intracellular Ca2+ in modulation of tight junction resistance in A6 cells. *Am. J. Physiol.* 266:F775–F784.

Kniesel, U., and H. Wolburg. 2000. Tight junctions of the blood-brain barrier. *Cell. Mol. Neurobiol.* 20:57–76.

Lacaz-Vieira, F. 1986. Sodium flux in the apical membrane of the toad skin: aspects of its regulation and the importance of the ionic strength of the outer solution upon the reversibility of amiloride inhibition. *J. Membr. Biol.* 92:27–36.

Lacaz-Vieira, F. 1997. Calcium site specificity - early Ca^{2+}-related tight junction events. *J. Gen. Physiol.* 110:727–740.

Lacaz-Vieira, F. 2000. Tight junction dynamics: oscillations and the role of protein kinase C. *J. Membr. Biol.* 178:151–161.

Lacaz-Vieira, F., and M.M. Jaeger. 2001. Protein kinase inhibitors and the dynamics of tight junction opening and closing in A6 cell monolayers. *J. Membr. Biol.* 184:185–196.

Lacaz-Vieira, F., M.M. Jaeger, P. Farshori, and B. Kachar. 1999. Small synthetic peptides homologous to segments of the first external loop of occludin impair tight junction resealing. *J. Membr. Biol.* 168:289–297.

Lacaz-Vieira, F., and B. Kachar. 1996. Tight junction dynamics in the frog urinary bladder. *Cell Adhes. Commun.* 4:53–68.

Levine, S.D., M. Jacoby, and A. Finkelstein. 1984. The water permeability of toad urinary bladder. I. Permeability of barriers in series with the luminal membrane. *J. Gen. Physiol.* 83:529–541.

Neter, J., and W. Wasserman. 1974. Applied Linear Statistical Models: Regression Analysis of Variance and Experimental Designs. Richard D. Irwin, Inc., Homewood, IL. 842 pp.

Ogata, K. 1998. Modern Control Engineering. Prentice Hall, Upper Saddle River, NJ. 997 pp.

Pak-Poy, R.F.K., and P. Bentley. 1960. Fine structure of the toad urinary bladder. *J. Exp. Cell. Res.* 20:235.

Peachey, L.D., and H. Rasmussen. 1961. Structure of the toad's urinary bladder as related to its physiology. *J. Biophys. Biochem. Cytol.* 10:529–553.

Schneeberger, E.E., and R.D. Lynch. 1992. Structure, function, and regulation of cellular tight junctions. *Am. J. Physiol.* 262:L647–L661.

Schultz, S.G. 1980. Basic principles of membrane transport. Cambridge Univ. Press, Cambridge. 143 pp.

Sten-Knudsen, O. 1978. Passive transport processes. *In* Membrane Transport in Biology. G. Giebisch, D.C. Tosteson, and H.H. Ussing, editors. Springer-Verlag, Berlin. 5–113.

Turner, J.R. 2000. Show me the pathway! Regulation of paracellular permeability by Na(+)- glucose cotransport. *Adv. Drug Deliv. Rev.* 41:265–281.

Walsh, S.V., A.M. Hopkins, and A. Nusrat. 2000. Modulation of tight junction structure and function by cytokines. *Adv. Drug Deliv. Rev.* 41:303–313.

Weyrick, R.C. 1975. Fundamentals of Automatic Control. McGraw-Hill Kogakusha, Tokyo. 397 pp.